A discrete dislocation model of Stage I fatigue crack growth and an analysis of Stage II to Stage I transition at low ΔK1

Véronique Doquet

A discrete dislocation model of Stage I fatigue crack growth and an analysis of Mode I to Mode II transition at low ΔK_I

V. Doquet

Laboratoire de Mécanique des Solides, UMR 7649 du CNRS, École Polytechnique, 91128 Palaiseau cedex, France

Abstract. Simulations of dislocations nucleation and glide ahead of a crystallographic mode II crack are performed for push-pull and reversed torsion . An influence of the normal stress on the friction of crack flanks, as well as on the condition for dislocation emission is introduced. The crack growth rates are deduced from the dislocation fluxes at the crack tip. A comparison between the loading modes is made. Taking into account the presence of grain boundaries, the repeated decelerations and sometimes the arrest that characterise Stage I crack growth are described by the model. An analysis of the transition from mode I to mode II crack growth observed at low ΔK_I in single crystals is proposed.

1.INTRODUCTION

In the first stage of their development, fatigue cracks are driven by the cyclic shear, but their growth rate is influenced by the normal stress: it is increased by an opening stress and reduced by a compressive one. The absence of an opening stress in torsion is often considered responsible for slower stage I growth and longer fatigue life compared to push-pull, for equivalent strain ranges [1]. The first aim of this work is to suggest mechanisms by which the normal stress could influence Stage I crack growth and illustrate them through micromechanical simulations. The second aim is to model the interactions of Stage I cracks with microstructural obstacles and the resulting irregularities in the crack growth kinetics. The third aim is to analyse the transition from stage II to stage I observed during push-pull tests on single crystals at low ΔK_I.

2.A BRIEF DESCRIPTION OF THE MODEL FOR UNCONSTRAINED SLIP

Stage I fatigue cracks grow along localized slip-bands. They are submitted to either pure shear loading in torsion or combined opening and shear in push-pull. But plasticity - that is dislocation nucleation and glide - is related only to the shear components and is restricted to the slip band colinear to the crack, otherwise (that is : if noncoplanar slip is activated) there is a transition towards Stage II propagation.

In the simulations, only mixed mode I+II loading has been considered. The dislocations that are emitted from the crack tip along the coplanar slip plane thus have a pure edge character. They are supposed to be perfect dislocations, but cross slip is not envisaged. In a first approach, decribed in details in [2], no obstacle to dislocation glide was considered. In a second phase, grain boundaries are introduced.

The cyclic loading path is followed by incremental time steps, Δt, small enough for the velocity of each dislocation to be considered constant over Δt. The nominal stress intensity factors for a Stage I crack of length 2a lying along the critical plane (i.e. the plane where the shear stress range is maximum) are calculated at each time-step as:

$$K_I = \sigma_{ncp}\sqrt{\pi a} \text{ when } \sigma_{ncp} \geq 0 . \quad K_{II}^{nom} = \tau_{cp}\sqrt{\pi a} \qquad (1)$$

where σ_{ncp} and τ_{cp} are the current values of the normal stress and shear stress on the critical plane . Since real Stage I cracks are not straight, allowance has to be made for asperity-induced friction that tends to reduce the crack driving force, and is either enhanced or reduced by a compressive (respectively tensile)

normal stress . Experimental information concerning crack flanks frictional interactions for cracks loaded in mode II, in presence of a static normal stress, has been obtained through combined tension and torsion tests performed inside a scanning electron microscope on precracked tubular specimens of maraging steel [2]. An attempt is made here to reproduce qualitatively these experimental data through empirical equations. The effective mode II stress intensity factor is thus calculated, assuming that a uniform, normal-stress-dependent friction stress, c, exists along the crack flanks:

$$K_{II}^{eff} = K_{II}^{nom} \pm c\sqrt{\pi a} \qquad (2)$$

$$c = c_0.\exp(-k_+.\sigma_{ncp}) \text{ if } \sigma_{ncp} \geq 0$$

with

$$c = c_0.\exp(-k_-.\sigma_{ncp}) \text{ if } \sigma_{ncp} \leq 0 \qquad (3)$$

c_0 characterises the friction stress in the absence of any normal stress and is thus related to the tortuosity of the crack path . k_+ and k_- are two constants, the latter connected with the friction coefficient of the material. The simulations described below have been performed with $k_+ = 0.057$, $k_- = 0.014$ (c is divided by one hundred for σ_{np} = 80MPa but is multiplied by three only for σ_{np} = -80MPa consistently with experimental data reported in [2]). The sign affecting the second term in (2) depends on the loading (-) or unloading (+) situation. Figure 1 shows how K_{II}^{nom} and K_{II}^{eff} vary in time during a reversed torsion and a push-pull cycle described respectively by: $\tau = \tau_0.\sin\omega t$ and $\sigma = \sigma_0.\sin\omega t$ with $\sigma_0 = 2\tau_0$ (equivalent stress ranges in the sense of Tresca) assuming that the crack lies along the maximum shear stress plane in each case. Note that ΔK_{II}^{nom} is the same in both cases. In push-pull , $K_{II,max}^{eff}$ is higher than in torsion, but the effective loading cycle is asymetrical, due to enhanced friction in the compressive part of the cycle.

The critical mode II stress intensity factor for the emission of a coplanar edge dislocation from the crack tip, which depends on the mode mixity parameter $\psi = \arctan(K_{II}/K_I)$, is then calculated , using the expression given by Sun, Beltz and Rice [3]:

$$K_{II}^{nucl} = \sqrt{\frac{2\mu}{(1-\nu)}[\gamma_{us}^{s} - \alpha.(\gamma_{us}^{u} - \gamma_{us}^{s})(\frac{\pi}{2} - \psi)]} \qquad (4)$$

where α , γ_{us}^{u} and γ_{us}^{s} are material parameters estimated by atomic models (density functional theory or embedded atom method) and tabulated in [3] for a few materials ($\gamma_{us}^{s}/\gamma_{us}^{u}$ and α are approximately 0.866 and 1.2, respectively, for Al and Ni). Since $\gamma_{us}^{u} > \gamma_{us}^{s}$, equation (4) predicts a lower threshold stress intensity factor for dislocation nucleation when an opening stress is present. This is not the case in torsion, for which $\psi = \frac{\pi}{2}$. For push-pull, $\psi = \frac{\pi}{4}$ during the tensile stage, but $\psi = \frac{\pi}{2}$ in the compressive stage, since K_I is then zero . For Al and Ni, equation (4) thus gives a nucleation stress intensity factor in the tensile stage of the push-pull cycle that is 92% of its value in torsion or in the compressive part of the cycle .

The shear stress on each dislocation in the plastic zone is then evaluated as:

$$\tau_i = \frac{K_{II}^{eff}}{\sqrt{2\pi x_i}} - \frac{\mu b_i}{4\pi(1-\nu)x_i} - \sum_{j \neq i} \frac{\mu b_j}{2\pi(1-\nu)}\sqrt{\frac{x_j}{x_i}}.\frac{1}{x_j - x_i} + \tau_{cp} \qquad (5)$$

in which the first three terms represent, respectively, the crack tip stress, the image stress and the stress of other dislocations. The last term is the far field term, negligible for dislocations located very close to the crack tip, but more important for leading dislocations, when the size of the plastic zone is a relatively large fraction of the crack size. In the following, however, the size of the plastic zone will never exceed 0.2a, so that equation (5) may be considered a reasonable approximation. The velocity of each dislocation is then calculated as:

$$v_i = v_0.\text{sign}(b_i).\text{sign}(\tau_i).\langle|\tau_i| - \tau_f\rangle^m \qquad (6)$$

where $\langle x \rangle$ is zero if $x \leq 0$ and x otherwise. τ_f is the resistance to dislocation glide when slip is not constrained by a grain boundary. For the simulations described below, τ_F varied between 20 and 90MPa. Typical values of v_0 and m for F.C.C. metals.(13ms^{-1} and 0.88, respectively) were chosen.

The new position of each dislocation is then deduced, and annihilation criteria are checked: if a dislocation comes close enough to the crak tip or if the distance between two dislocations with opposite signs becomes less than 16nm, they are removed from the simulation.

The real mode II stress intensity factor, allowance made for crack tip shielding by the dislocation stress field [4], is then evaluated as:

$$K_{II}^{tip} = K_{II}^{eff} - \sum_{i=1}^{n} \frac{\mu b_i}{(1-\nu)\sqrt{2\pi x_i}} \qquad (7)$$

The dislocation emission criterion:

$$K_{II}^{tip} \leq -K_{II}^{nucl} \text{ or } K_{II}^{tip} \geq K_{II}^{nucl} \qquad (8)$$

is then checked to decide whether a negative or positive dislocation can be emitted.

This sequence is repeated until the second cycle is completed. Then, the crack growth rate per cycle is deduced from the dislocation flux as follows. The crack is considered to grow by one Burgers vector each time a pair of positive-negative dislocation has been emitted or when a dislocation returns to the crack tip. In the latter case, it is assumed that even though the crack tip geometry before the dislocation nucleation is, in principle, recovered when this dislocation comes back, the free surface increment created at nucleation, that has been exposed to environment and gas adsorption in the meantime, cannot be rewelded. Anyway, both events correspond to some cyclic plastic flow at the crack tip and should thus contribute to its growth.

3.RESULTS FOR UNCONSTRAINED SLIP

The dislocation dynamics during push-pull and reversed torsion loadings is analysed in details in [2]. Only global results will be given here. Simulations have been carried out for reversed torsion and push-pull for various loading ranges and various friction stresses c_0. The results are drawn on a bilogarithmic plot of da/dN versus ΔK_{II}^{nom} on Fig.2 (curves labelled B, E, F). For torsional loading, the effective loading is fully reversed, and no opening stress affects the threshold for dislocation emission, so that the calculated growth rates follow a very simple equation:

$$\frac{da}{dN} = \frac{(1-\nu)}{4.\mu.b.\tau_f}.(\Delta K_{II}^{eff2} - 4.K_{II}^{nucl2}) \qquad (9)$$

in which K_{II}^{nucl} is the emission threshold in pure shear. The threshold for propagation is thus $2K_{II}^{nucl}$ in that case. Quite similarly to closure effects for mode I propagation, the friction stress along the crack flanks shifts the da/dN versus ΔK_{II}^{nom} curve compared to the "intrinsic" curve corresponding to zero friction.

Comparing the curves labelled A and B, it appears that even without friction, the crack growth rate is higher in push-pull than in reversed torsion, but the difference, appreciable for small loading ranges, vanishes as the loading range increases. This is probably because close to the threshold, the critical stage for crack propagation is dislocation **nucleation**, which is made easier by the opening stress, in push-pull, whereas for higher loads, nucleation is no more critical, but **reverse dislocation glide**, more natural under reversed torsion because of the symetry of the effective loading, is. According to this trend, the ratio between torsional and tensile fatigue lives should thus increase as the loading range decreases. This corresponds to experimental observations [1] and it is thus very encouraging. When crack flanks friction is introduced, the difference in Stage I kinetics between the two loading modes is amplified.

4.INTERACTIONS WITH MICROSTRUCTURAL OBSTACLES

4.1.Influence of an impenetrable obstacle

If there is an impenetrable obstacle ahead of the crack, the dislocations emitted pile up there, and as the crack propagates towards the obstacle, the shielding effect due to the pile up is stronger and stronger. The increment of K_{II}^{eff} necessary for the emission of a new dislocation is thus higher and higher. and there are fewer dislocations emitted, even though $\Delta K_{II}^{nominal}$ increases, so that the crack decelerates. When the crack tip is finally so close to the obstacle (say, less than the core radius of a dislocation) that there is not enough

space for a single dislocation loop to expand from the tip, the emission criterion of equation (8) is not applied any more. The crack is thus predicted to stop if the obstacle has not yet been overcome by dislocations when the crack tip is closer than a few nanometers.

Simulations of stage I growth for two constant stress ranges and thus increasing ΔK_{II}^{nom} were performed, in reversed torsion, for a crack approaching an impenetrable obstacle. The friction stress, τ_f was 30MPa Figure 3 shows the evolution of the calculated growth rate. For both cases illustrated, $\tau_{cp,max} > \tau_f$, so that the crack-tip plastic zone hits the obstacle for each crack length considered. But for the smallest stress range, the number of dislocations emitted is small, so that down to 5μm distance from the obstacle, the rise of the shielding term in equation (7) is slower than the increase in K_{II}^{eff}, and the crack is able to accelerate, in spite of its constrained plastic zone. For the highest stress range , the rise of the shielding term compensates that of K_{II}^{eff} at the beginning, and then exceeds it, whence the constant and then decreasing growth rate.

4.2.Influence of grain boundaries

Grain boundaries (G.Bs.) are generally not impenetrable to dislocations. They can be sinks for dislocations as well as sources. Dislocations are assumed to pile-up on a G.B, until the shear stress on the leading dislocation reaches a value allowing slip transfer into the next grain, on a slightly misoriented plane. The tilt of the crack path beyond the G.B is not taken into account explicitely, but some of it is modelled through the roughness-induced friction stress. The critical shear stress for slip transfer, $\tau_{G.B.}$, should depend on the crystallographic misorientation of the adjacent grains, and on the angle of incidence of the slip plane on the G.B. plane.

Simulations of stage I growth at a constant stress range ($\Delta\tau/2$=36.5MPa) have been performed, in reversed torsion, for a crack of initial half length, a = 105μm, in a polycrystal with a 15μm mean grain size and a 30MPa friction stress. The calculated crack growth rates are plotted versus the crack length on Fig.4, for two values of the critical stress for slip transfer at grain boundaries, $\tau_{G.B.}$, small enough to allow the crack to cross the grain boundaries. The size of the plastic zone, in microns, is indicated for each point . It can be seen that the condition for slip transfer beyond the first G.B.is met earlier and earlier in successive grains because of the increase in ΔK_{II}^{nom} associated with an increase in the number of dislocations piled-up against the G.B.. But this does not produce a sudden acceleration, since slip transfer is progressive: the plastic zone may well extend over the G.B. but a substantial fraction of the emitted dislocations may still be withheld by the G.B. and have a strong shielding effect. For example, for $\tau_{G.B.}$ =400MPa, the crack growth rate for a=164μm is smaller than for a=160μm, even though the plastic zone is larger, since in the former case, only 3 of the emitted dislocations have been transmitted to the second G.B and 8 of them remained stacked in a 1μm wide zone ahead of the crack tip. It also appears that each time the crack tip enters a new grain, there is a sudden acceleration. The magnitude of this acceleration depends on $\tau_{G.B.}$, since the stronger $\tau_{G.B.}$ is, the higher the fraction of emitted dislocations withheld by the first G.B., and thus the larger the decrease in dislocation shielding when the crack passes the G.B..

4.3. Influence of the loading mode

It had been observed, on a Co45Ni alloy, that for equivalent stress ranges, it takes approximately twice as long for microcracks, **once initiated**, to cross the first G.B. encountered in reversed torsion than in push-pull [1] but it was not clear whether this came merely from a slower transgranular growth rate, or if the interaction between microcracks and G.Bs. was stronger in torsion. The present simulations throw some light on that point. Figure 5 compares the stress concentrations due to the emitted dislocations, at 1μm from the G.B. in the next grain, for a crack propagating toward a G.B., for reversed torsion and push-pull loadings of equivalent stress ranges. The stress concentration in the next grain is much higher in push-pull, because the opening stress increases K_{II}^{eff} and decreases K_{II}^{nucl}, so that many more dislocations are emitted than in torsion. Slip transfer is thus easier, which obviously facilitates G.B. crossing, not to mention the possibility to activate non coplanar slip systems in the next grain, that would be able to shield the mode I singularity, contrary to coplanar slip. The slower development of microcracks in torsion thus probably results from stronger interactions with the microstructure as well as from the lower transgranular growth rate illustrated in Fig.2.

5.TRANSITION FROM MODE I TO MODE II PROPAGATION

Several authors, among which Petit et al.[5] report transitions from mode I to mode II fatigue crack growth observed during push-pull tests on single crystals at decreasing ΔK_I, when the mode I growth rate is about 10^{-10}m/cycle. An equivalent transition from true mode I to "crystallographic mode I" is also observed in polycrystals close to the threshold. This transition is analysed below in terms of dislocation dynamics for the ideal case where mode I crack growth is due to dislocation emission on two symetrically inclined slip planes. For an FCC structure, this means that the crack plane is of (100) or (110) type, and that the angle between the crack plane and slip planes is $\theta = 54°73$ or $\theta = 35°26$ respectively. The threshold stress intensity factor for the emission of dislocations parallel to the crack front on inclined slip planes has been estimated by Sun et al.[3], neglecting tension-shear coupling ($\gamma_{us}^u = \gamma_{us}^l$) as: $K_{I,emission} = \sqrt{\frac{16\mu\gamma_{us}}{(1-\nu)(1+\cos\theta)\sin^2\theta}}$ that is: $3.635K_{II,emission}$ for $\theta = 54°73$ and $2.76K_{II,emission}$ for $\theta = 35°26$, where $K_{II,emission} = \sqrt{\frac{2\mu\gamma_{us}}{(1-\nu)}}$ is the threshold for coplanar emission in mode II. Riemelmoser et al. [6] have shown that since mode I is not a reversed loading, $K_{I,max}$ must exceed $1.3K_{I,emission}$ for some dislocations to come back to the crack tip, aided by the repulsive force from previously emitted dislocations. So, during push-pull tests at decrasing ΔK_I, when $K_{I,max}$ becomes less than $1.3K_{I,emission}$, the crack can no more propagate in mode I for lack of cyclic plasticity at its tip. But assume it bifurcates on either of the two active slip planes. The mode II stress intensity factor at the tip of the small branch, during the tensile stage of the cycle is, according to Amestoy et al.[7], $k_{II}^* = F(\theta)K_I$, where $F(\theta)=0.358$ for $\theta = 54°73$ and 0.272 for $\theta = 35°26$. Thus $k_{II}^* = 1.3F(\theta)K_{I,emission} = 1.284K_{II,emission}$ in both cases, which is largely sufficient for coplanar dislocation emission. In addition, contrary to mode I loading, the shear loading on the branch of length 2s is partially reversed: during the compressive stage of the cycle, the main crack is closed and $K_I = 0$, but k_{II}^* can be roughly estimated as if the main crack did not exist as: $k_{II}^* = \sigma\sin\theta\cos\theta\sqrt{\pi s} = 0.47\sigma\sqrt{\pi s}$, where σ is the applied compressive stress. This change in sign of k_{II}^* should allow some dislocations to come back to the crack tip and thus propagation along this slip plane.

6.CONCLUSIONS

Simulations of Stage I fatigue crack growth by dislocations emission/annihilation at their tip, taking into account their interactions with grain boundaries have been developped. The existence of a threshold for crystallographic mode II crack growth, even in single crystals, was predicted. The influence of friction stresses along the crack flanks was illustrated: it shifts the da/dN versus ΔK_{II}^{om} curve compared to the "intrinsic" curve without friction. The periodic decelerations, sometimes leading to crack arrest typical of microstructure-sensitive Stage I propagation were simulated. Stage I is predicted to be slower under reversed torsion than under push-pull for equivalent stress ranges in the sense of Tresca, because of slower transgranular growth rate and more difficult G.B. crossing. The ratio of torsional to tensile fatigue lives should depend on the roughness of Stage I cracks and the frictional properties of the material. An analysis of the transition from mode I to mode II propagation observed in single crystals as well as from true mode I to "crystallographic mode I" in polycrystals at low ΔK_I has been proposed.

References

[1] V.Doquet , Fat.Fract.Engng.Mater.Struct.**20**, 227-235 (1997)
[2] V.Doquet, Fat.Fract.Engng.Mater.Struct.**21**, 661-672 (1998)
[3]Y. Sun, G.E.Beltz and J.R.Rice, Mat. Sci. Eng.,**A170**, 67 (1993)
[4] I.H.Lin and R.Thomson, Acta Metall.**34**, 187 (1986)
[5] J.Petit J., K.Kosche, H.J. Gudladt, Scripta Met. et Mat. **26**, 1049-1054 (1992)
[6] F.O.Riemelmoser , R.Pippan , H.P.Stüwe, Int.Journ.Fract. **85**, 157-168 (1997)
[7] M.Amestoy, H.D.Bui, K.Dang Van, Advances in Fracture Research, ICF5, 1, 107-113 (1981)

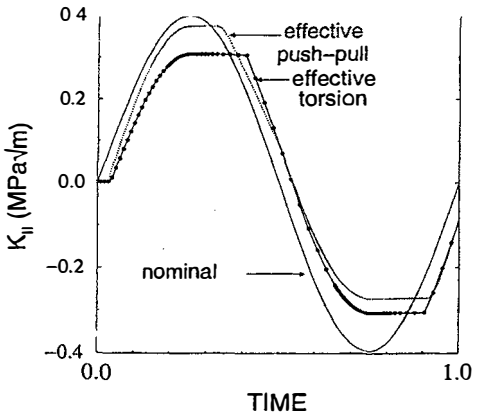

Fig.1 Evolution of nominal and effective K_{II} for a crack lying along the maximum shear stress plane under reversed torsion and push-pull loadings of equivalent amplitude in the sense of Tresca.

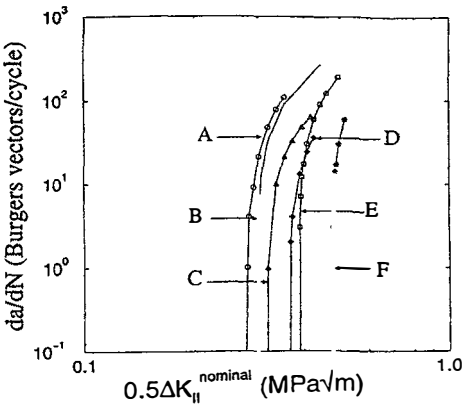

Fig.2 Computed growth rates versus nominal ΔK_{II} for (A) push-pull, no friction (B) reversed torsion, no friction (C) push-pull, c_0=5MPa (D) push-pull, c_0=10MPa (E) reversed torsion, c_0=5MPa (F) reversed torsion, c_0=10MPa

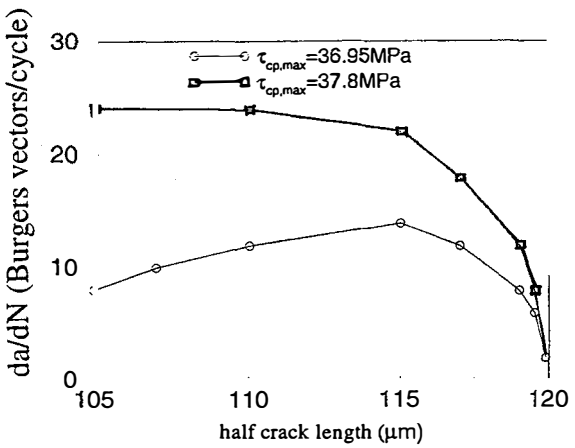

Fig.3 Evolution of the growth rate of a torsional stage I crack (initial half length 105μm) propagating toward a strong obstacle, initially 15μm away.

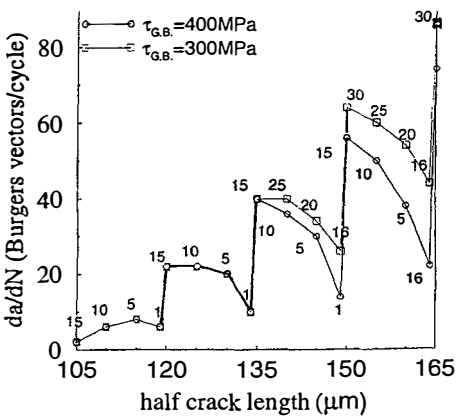

Fig.4 Evolution of the growth rate of a torsional stage I crack in a polycrystal of 15μm mean grain size, for various critical stresses for slip transfer at G.Bs.

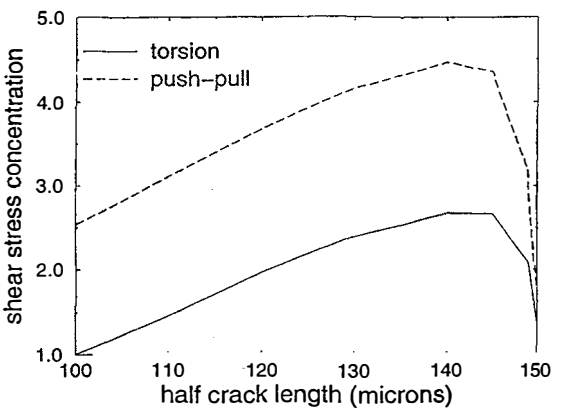

Fig.5. Stress concentration in the next grain, at 1μm from the G.B., due to the dislocations piled-up at the G.B., versus the distance between crack tip and G.B.